Excitation of cyclotron resonances from random fluctuations of stellarator windings

E. Drakakis, D. Karabourniotis, and C. A. Kapetanakos
Institute of Plasma Physics, University of Crete, Iraklion, Crete, Greece
(Received 10 July 1995; revised manuscript received 11 September 1995)

We have investigated the effect of random fluctuation of stellarator windings in a modified betatron accelerator configuration on the dynamics of the beam centroid by solving numerically the equations of motion. Our results show that random displacements of the windings by a few millimeters produce field errors that excite the cyclotron resonance modes that efficiently direct most of the input energy from the axial to transverse direction. These random displacements become completely harmless when their maximum amplitude is reduced to ± 0.5 mm. When even such small displacements cannot be attained, the errors that are produced from the mispositioning of the windings may become benign by using a crowbar on the current of the windings before the critical resonance is reached. At $\ell = m$ (≈ 6 in our case), where ℓ is the value of the cyclotron mode and m is the value of field periods in the device, i.e., when the frequency of the cyclotron mode is equal to the frequency of the strong focusing mode, the beam centroid encounters a potent resonance and locks in at it, even when the windings are located at their ideal positions. If crossing of the $\ell = m = 6$ mode is desired, using a crowbar on the strong focusing field may be the only remedy.

PACS number(s): 29.27.Bd, 29.20.Fj, 41.75.Ht

I. INTRODUCTION

The modified betatron accelerator (MBA) is a high current, recirculating, accelerator with high effective accelerating gradient. Its improved current carrying capability is due to the addition of two magnetic fields, a toroidal B_θ [1] and a strong focusing [2,3], to the vertical B_z field of the conventional betatron [4].

The development of the MBA at the Naval Research Laboratory (NRL) lasted several years and furnished valuable information on the various critical physics issues of the concept [5,6]. During the last phase of its operation the trapped electron current in the NRL device routinely exceeded 1 kA and the peak energy was above 20 MeV [6]. All the electron rings in the NRL accelerator were formed by an externally injected electron beam of energy between 0.5 and 0.6 MeV, produced by a high impedance injector accelerator. A smaller MBA at the University of California, Irvine [7] also obtained interesting results. However, the majority of electron rings in the Irvine accelerator were formed by runaway electrons and not by an injected beam.

The experimental results indicated that the beam current in the NRL device decays slowly during the acceleration phase, starting approximately at $\tau_x = 200$ μsec. There is extensive experimental evidence suggesting [5,6] that the bleeding of the beam current is caused by the cyclotron resonances. The time τ_x at which the bleeding starts, as monitored by the initial appearance of the x-ray signal, is independent of the trapped beam current but depends on the value of B_θ and dB_z/dt [6].

Following the successful demonstration of acceleration, a concerted effort was made by the NRL group to locate and eliminate or reduce the field disturbances that may excite the cyclotron resonances. Initially, the effort was focused on the field errors associated with B_z, B_θ, the magnetic flux, and the portholes. Reduction in many of these field errors together with operation at higher B_θ and strong focusing field led to improved performance of the device [6].

However, the problem of the slow losses of the beam still persisted after the reduction of field errors. During the last phase of the project, the NRL group investigated numerically and for a short period of time the effect on the beam from random fluctuation in the stellarator windings. They found that such fluctuations have a pronounced effect on the beam dynamics and may cause the observed beam losses.

Recently, using the NRL code, we have investigated the effect on the beam centroid of randomly positioned stellarator windings under a wide range of parameters. Our results indicate that although the numerically predicted τ_x shows the same trend, upon B_θ and dB_z/dt, as the τ_x of the experiment, their values are substantially different.

Therefore the mispositioning of the strong focusing windings alone cannot account for the observed beam losses. In addition, we found that these random fluctuations are not detrimental to the modified betatron concept, because their negative impact can be completely eliminated by positioning the windings with an accuracy of approximately ± 0.5 mm or by using a crowbar on the winding current just before the troublesome resonance is reached. It should be noticed that the NRL group designed and constructed a strong focusing system in which the strong focusing windings were positioned with an estimated accuracy of $\approx \pm 0.5$ mm. Unfortunately, the fabrication of the system was not completed on time and thus was never installed and tested.

II. ORIGIN OF FIELD ERRORS AND NUMERICAL MODEL

Although the effective accelerating gradient of the MBA is high, its actual gradient is rather low. Thus in order to reach even modest peak energies the beam electrons perform a large number of revolutions. As a result the electron beam is sensitive to field errors. These field errors may excite various resonances, such as the cyclotron resonances, which increase the transverse velocity of the electrons and may drive them to the wall of the vacuum chamber.

The NRL research staff has investigated several sources of field errors, including coil misalignment, coil discreteness, portholes in the vacuum chamber, eddy currents induced by the magnetic flux on the support structure of the device and various coil feeds. Reduction of the various field disturbances led to higher peak energies and, in general, improved performance of the device. However, the beam losses continued to persist. This led the NRL staff to investigate errors that are produced from the mispositioning of the stellarator windings [6].

In the computer model, the magnetic field of the stellarator windings is computed from the Biot-Savart law using filaments of infinitesimal radius. The helical filaments are approximated by series of discrete segments of equal but adjustable length. For most of the runs the segment length was selected to be 10.45 cm. The ends of each segment are randomly positioned within a cube of adjustable volume.

The vertical magnetic field is numerically computed from nine pairs of circular coils that are symmetrically located with respect to the midplane of the device, in positions that are the same as those of the experiment. The temporal profile of the field is sinusoidal with period of 10.4 msec and a peak value that typically is 1150 G. The flux condition is adjusted by varying the number of coils. The model assumes a smooth toroidal magnetic field that varies as $1/r$. In addition to the external magnetic fields, the code includes induced fields from the wall of the vacuum chamber. However, the self-fields of the beam have been neglected. Inclusion of such fields would require a fully three-dimensional (3D) computer simulation code, which is not currently available in our Institute. Only such a code can provide reliable information on the dynamics of individual particles inside the beam and help in the detailed understanding of the observed x-ray spectra.

Therefore our model is addressing only the dynamics of the beam centroid and as such is of limited usefulness. Still, the results can be useful in predicting trends and also for providing guidance on the necessary steps to correct the problem.

III. NUMERICAL RESULTS

A. Basic run

Figure 1 shows selected frames from a long computer run. The left-hand side of this figure shows the projection

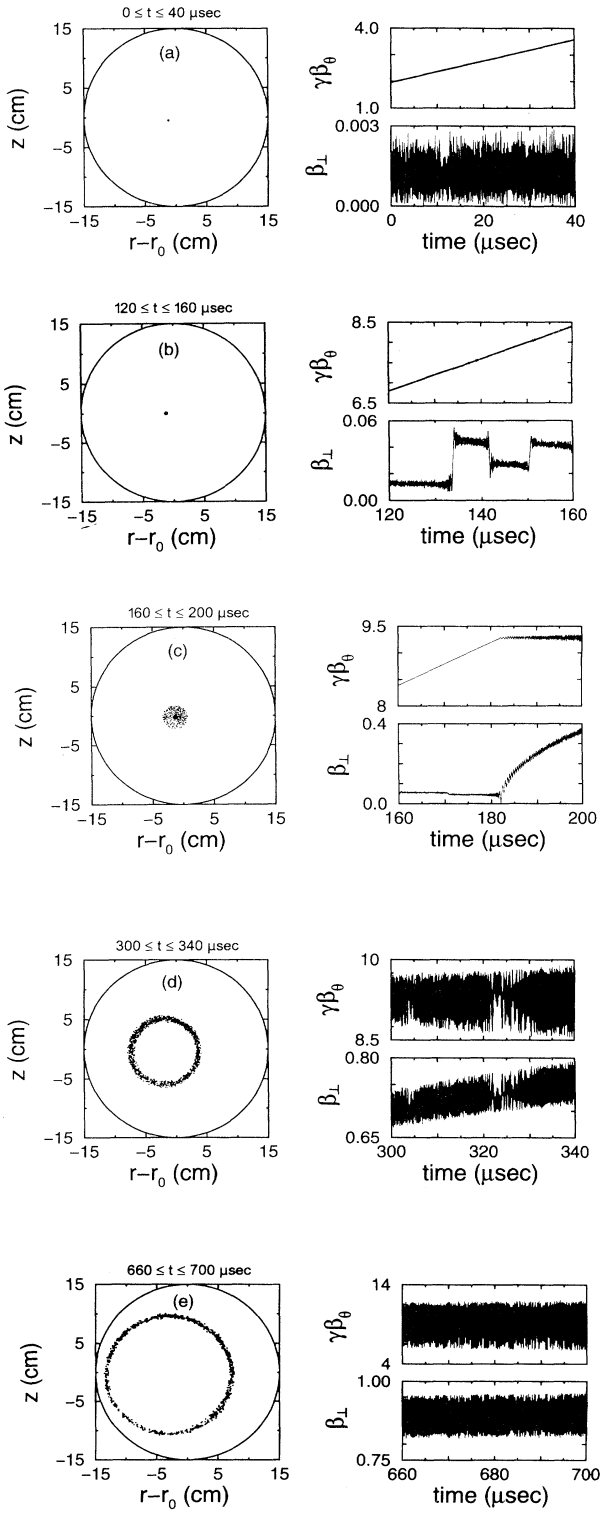

FIG. 1. Selected frames of a run for the parameters listed in Table I. The left-hand side shows the beam centroid orbit in the x-z plane. The right-hand side shows the time profile of $\beta_\perp$ and $\gamma\beta_\theta$. In (b), the beam crosses different resonances while in (c) it locks at ≈ 182 μsec in the $\ell = 19$. In (d) and (e) the radius of the fast motion increases continuously as $\beta_\perp$ grows and the beam centroid drifts radially inward.

of the beam on the x-z vertical plane for the time interval indicated in each frame. The right-hand side shows the temporal evolution of the normalized transverse velocity $\beta_\perp \equiv (\beta_r^2 + \beta_z^2)^{1/2}$ and the normalized toroidal momentum $\gamma\beta_\theta$, where γ is the relativistic factor and β_θ is the normalized toroidal velocity. The reference particle is injected with initial $\gamma_0 = 2.2$ and is situated on the magnetic axis, which is located at a distance $r = 98.9$ cm from the major axis. Its initial position is selected to be consistent with the experimental observation, which indicates that the beam spirals from the injection position to the magnetic axis within about 1 μsec. The rest of the parameters are listed in Table I.

In Fig. 1(b) the beam reaches the $\ell = 24$ resonance at $t \approx 132$ μsec. Its transverse velocity grows quickly and then saturates and remains constant until the beam reaches the next resonance. The product $\gamma\beta_\theta$ continues to increase. This is the Fresnel regime [8] which is characterized by bounded transverse velocity $\beta_\perp$. In Fig. 1(c) the beam reaches the $\ell = 19$ resonance at $t \approx 182$ μsec, and its transverse velocity increases continuously while $\gamma\beta_\theta$ remains constant, following an initial rapid rise. This is called the "lock-in" regime, in which all the energy from the accelerating field goes to the transverse motion ($\beta_\perp$) instead of to toroidal motion (β_θ). The Larmor radius of the fast motion increases continuously as the transverse velocity grows and simultaneously the beam centroid drifts radially inward with a speed that is ≈ 0.05 mm/μsec, as is apparent in Figs. 1(d) and 1(e). Eventually, the beam hits the wall at $t = 816$ μsec.

When the beam locks at a resonance, $\gamma\beta_\theta$ remains approximately constant during acceleration and thus its major radius should shrink as the vertical magnetic field rises with time. The observed shrinkage of its major radius is substantially smaller than that expected, because the growing transverse velocity causes a radial drift [9] that reduces the inward motion of the beam. It can be shown that in the lock-in regime the final normalized energy $\gamma_{\rm fin}$ of the reference electron is given approximately by

$$\gamma_{\rm fin} = \left(\gamma_{\rm in}^2 + 2(\gamma\beta_\theta)_{\rm fin}\frac{\langle r\rangle}{c}[\Omega_{z\rm fin} - \Omega_{z\rm in}]\right)^{1/2},$$

where $\Omega_{z\rm fin}$ and $\Omega_{z\rm in}$ are the final and the initial cyclotron frequencies of the vertical magnetic field and $\gamma_{\rm in}$ is the initial normalized energy. This equation is based on the assumption that the major radius r of the centroid remains approximately constant and equal to $\langle r\rangle$ during the acceleration process.

The majority of the computer runs reported in this paper were taken with a time step of 20 psec. By reducing the time step to 10 psec, we have not observed any noticeable difference in the numerical results. However, this is not the case with a time step of 30 psec. Obviously, the optimum time step of 20 psec has to be modified when the value of the toroidal magnetic field is changed.

The length of segments does not appear to have a pronounced effect on the results, at least within the range of parameters tested. By decreasing the segment length from 10.45 cm to 3.48 cm the reference electron entered the lock-in regime at $\ell = 22$ instead of at $\ell = 24$ and the beam lifetime increased by less than 20%. The effect was even smaller when the length of the segment increased from 10.45 cm to 20.90 cm.

TABLE I. Parameters of the run shown in Fig. 1.

Major radius r_0	100 cm
Torus minor radius a	15.2 cm
Toroidal magnetic field $B_{\theta 0}$	3 kG
Vertical magnetic field B_{z0}	34 G
Relativistic factor γ_0 (at injection)	2.2
Flux condition	1.98
Minor radius of windings	23.4 cm
α	0.03 cm^{-1}
Current in the windings	25 kA
Length of helical segments	10.45 cm
Maximum random displacement of the segments	± 4 mm
dB_z/dt (at injection)	0.69 G/μsec
Initial radial position $(r - r_0)$	-1.1 cm
Initial vertical position z	0.0 cm
Initial transverse velocity $v_\perp$	0

In contrast, the results are sensitive to the value of the toroidal magnetic field. As B_θ increases the reference particle locks at lower ℓ value and its lifetime becomes longer. This is consistent with the experimental results [6]. However, the numerically computed time for the reference electron to hit the wall of the vacuum chamber is longer than the time τ_x at which the x-ray signal initially appears in the experiment. It is likely that additional field errors are present in the experiment that shorten the beam lifetime. The rapid oscillations of $\beta_\perp$ and $\gamma\beta_\theta$ that are very pronounced in Figs. 1(d) and 1(e) have a frequency equal with the frequency of the toroidal magnetic field and are caused by the $1/r$ dependence of B_θ.

Similarly, the results are sensitive to the value of the flux condition. We made a run with flux condition ≈ 2.3, keeping the rest of the parameters the same as those of Table I. At the higher flux condition the electron locked in at $\ell = 23$ and its lifetime decreased. Even more importantly, it drifted radially outward with a speed that is approximately 0.17 mm/μsec. Apparently, as a result of the mismatch of the flux and the vertical magnetic field, the energy of the reference electron increases faster than the local field and thus it obtains an outward drift that exceeds the inward drift that occurs at flux condition ≈ 2.0.

As expected, lesser winding displacements result in smaller beam disturbances. The effect is not very pronounced when the maximum winding displacement is reduced from ± 4 mm to ± 2 mm. The initial lock-in resonance ℓ value remained unchanged and the beam lifetime was slightly longer. For ± 1 mm displacement the initial lock-in resonance value was reduced from $\ell = 19$ to $\ell = 15$. Finally, at ± 0.5 mm the centroid crossed all the resonances up to $\ell = 6$ without locking in at any of them. Although the centroid locked in at $\ell = 6$ and remained frozen at this ℓ for the rest of its lifetime, this

effect is not related to the field errors produced by the small displacements of the stellarator windings, as it is discussed in the next section. At the flux condition of 2.3 and for ± 2 mm winding displacement, the reference electron does not stay locked at the same resonance during its entire lifetime when its initial radial position is reduced from -1.1 cm to -0.14 cm. Routinely, it moves in and out of the lock-in regime with occasional reduction in its transverse velocity. The initial lock-in resonance value also depends on the initial radial position of the centroid. Apparently, more work is needed to clarify the subtleties associated with the initial positions.

In all of our runs with winding displacement of ± 2 mm or greater, we have consistently observed that the reference electron initially locks in at $\ell = 24$, 23, or 19. In order to understand this result we have analyzed a typical field error that is produced from the random fluctuations of stellarator windings. Each of the three error components ΔB_r, ΔB_z, and ΔB_θ is the difference of the field component with displaced windings minus the corresponding component of the undisturbed system. The three components are shown in Fig. 2 as a function of the toroidal angle, at $r = 98.9$ cm and $z = 0$, when the current of the windings is 25 kA and their maximum displacement ± 4 mm.

Figure 3 shows the Fourier decomposition of the three components. It is apparent from Fig. 3(a) that the amplitude of the $\ell = 19$ is considerably higher than the amplitude of all adjacent modes. The same is true, although to a lesser degree, about modes 23 and 24. Therefore it is not surprising that the beam locks initially in one of these modes.

As expected, the amplitude of magnetic disturbances increases rapidly at positions closer to the windings. Specifically, at $r = 110$ cm the amplitude of some peaks

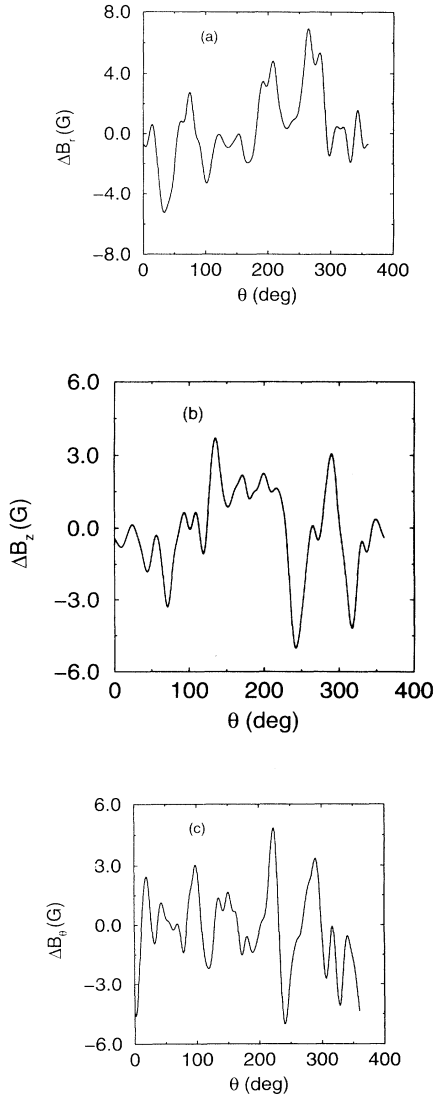

FIG. 2. The three error components ΔB_r, ΔB_z, and ΔB_θ (in gauss) of the stellarator field vs the toroidal angle θ, at $r = 98.9$ cm and $z = 0$ cm for 25 kA current in the windings and ± 4 mm maximum displacement.

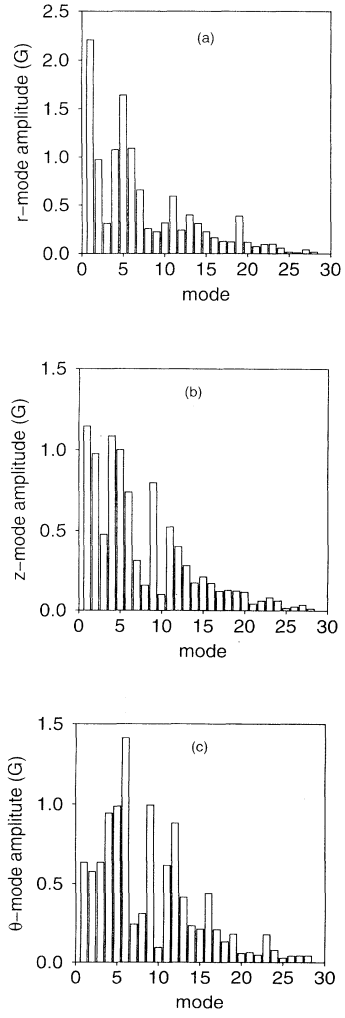

FIG. 3. Fourier decomposition of the three error components of Fig. 2.

is higher by a factor of 3 than those of Fig. 2. Even more pronounced is the rise of the amplitude of some high ℓ value modes. At $r = 110$ cm the amplitude of a few modes is higher by more than a factor of 10 than those shown in Fig. 3. Interestingly enough, the $\ell = 9$ and $\ell = 19$ become the dominant modes in the ΔB_θ spectrum with amplitude equal to 1.5 G.

B. Run without field error

We have made several runs with the windings in their ideal positions, i.e., without any displacement of the segments. Figure 4 shows a few selected frames from a typical run without displacement and with the rest of the parameters the same as those of Table I.

The results show that during the initial 710 μsec, i.e., until the reference electron reaches the threshold of the $\ell = 6$ resonance, (i) it remains at its initial position, (ii) its transverse velocity was no more than 0.1% of its total velocity, and (iii) it crossed all the resonances with $\ell > 6$ completely unscathed. Shortly after 710 μsec the beam centroid starts to obtain rapidly transverse velocity and the product $\gamma\beta_\theta$ saturates at ≈ 29.9. At this point the centroid locks in in the $\ell = 6$ resonance and remains locked until $t \approx 1003$ μsec, i.e., until it hits the wall of the vacuum chamber.

In a device with six field periods, i.e., $m = 6$, the cyclotron mode ω_{-+} and the strong focusing mode ω_{+-} [6] become equal at $\ell = 6$. Specifically, $(2\ell^2 - 1)/2\ell = 5.91$ and $\omega_{+-}/(\Omega_{z0}/\gamma) = m - \omega_B/(\Omega_{z0}/\gamma) = m - \Omega_{z0}/(2\Omega_{\theta 0}) = 6 - 1/12 = 5.91$. These expressions are valid when γ is high and thus the space charge can be neglected in all the terms, including the bounce frequency ω_B and $(B_\theta/B_z)^2 \gg 1$.

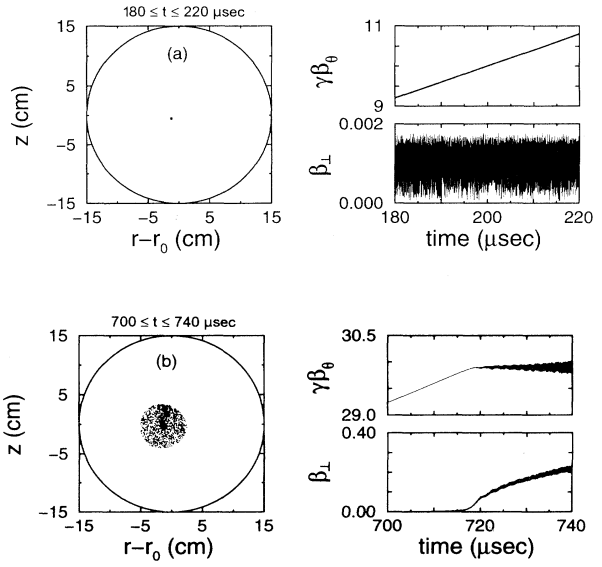

FIG. 4. Selected frames from a run without any displacement of the windings. The rest of the parameters are listed in Table I. In contrast to Fig. 1(c), the beam centroid crosses the $\ell = 19$ resonance without locking in, as it is apparent from the temporal frame of (a). Eventually the beam locks in at $\ell = 6$ at ≈ 720 μsec as can be seen from (b).

In a frame that rotates with $\omega_w/2 = \omega_{+-}/2$, a mismatched beam centroid will experience a harmonic driving force of frequency $\omega_w/2$. In the same frame the frequency of the cyclotron mode becomes $\omega_{-+} - \omega_w/2 = \omega_w/2$ [10]. Therefore it will be very difficult for the reference particle to cross the $\ell = 6$ and lower ℓ value modes, whenever its energy mismatch is not very small. An obvious remedy is to use a crowbar on the strong focusing field just before the beam reaches the $\ell = 6$ resonance.

C. Using a crowbar on the strong focusing field

The NRL results have unambiguously demonstrated that the strong focusing windings substantially improve the confining properties of the device at least for the first few hundred microseconds. As the beam energy increases, the importance of the space charge diminishes, making the winding less essential. Specifically, the self-field index n_s decays as γ_0^{-3} and the centroid self-field index decays initially as γ_0^{-3} and subsequently, after the wall current induced by the beam has decayed, as γ_0^{-1}. Furthermore, the strong focusing field index scales as γ_0^{-1}. Therefore using a crowbar on the current in the windings after the initial phase may have some definite benefits such as avoidance of the $\ell = 6$ resonance and elimination of possible field errors that are generated from the mispositioning of the windings.

In the code the crowbar action is initiated at $t = t_{\rm cr}$ and the strong focusing field varies as

$$\vec{B}(\rho, \phi, t) = \vec{B}(\rho, \phi) e^{-k(t - t_{\rm cr})}, \tag{1}$$

where ρ, ϕ are the spatial coordinates and k is the decay constant.

The value of k has been determined from the adiabatic condition

$$\frac{1}{B\omega_w} \left| \frac{\partial B}{\partial t} \right| \ll 1 \tag{2}$$

as follows.

Substituting (1) into (2), we obtain

$$\frac{k}{\omega_w} \ll 1. \tag{3}$$

Since $\omega_w \approx m(\Omega_{z0}/\gamma) \approx 18 \times 10^8$ sec^{-1}, an appropriate value of k is 1.8×10^8 sec^{-1}, i.e., the fields go to zero at about 100 nsec.

Figure 5(a) shows results from the numerical integration of orbit equations with the same parameters as the run of Fig. 1, but using a crowbar on the strong focusing field at $t_{\rm cr} = 165$ μsec. It is apparent from Fig. 5(a) that the reference electron did not lock in at $\ell = 19$. As a matter of fact, the beam centroid, as expected, crossed all lower ℓ values without suffering any adverse effect.

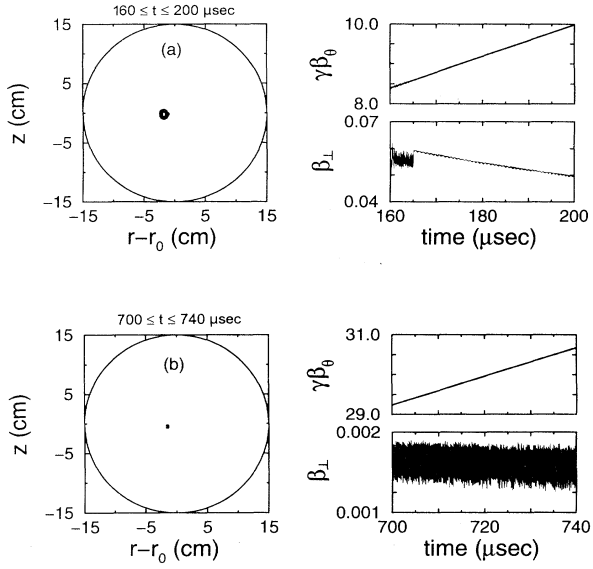

FIG. 5. The lock in can be avoided by using a crowbar on the current in the strong focusing windings. In (a) the use of the crowbar occurs at 165 μsec [compare with Fig. 1(c)] and in (b) at 705 μsec [compare with Fig. (4b)].

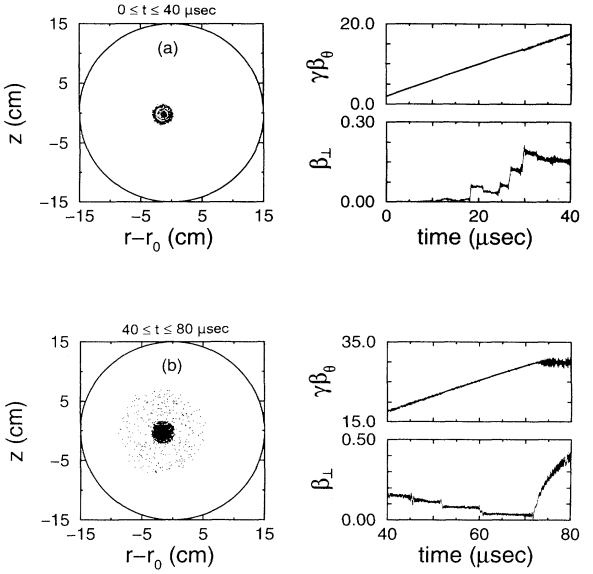

FIG. 6. Two consecutive frames from a run with acceleration rate 6.9 G/μsec. The rest of the parameters are listed in Table I. It is apparent from (a) that the beam centroid crosses all the $\ell > 6$ resonances without locking in. However, as it is manifested by (b), the centroid cannot cross the $\ell = 6$ even at such a high accelerating rate.

Figure 5(b) shows the results from a computer run with the same parameters as the run of Fig. 4(b), but using a crowbar on the strong focusing field at $t_{cr} = 705$ μsec. Clearly, the elimination of the driver made the $\ell = 6$ mode completely harmless.

D. Effect of higher acceleration rate

It is intuitively obvious and it has been demonstrated experimentally [6] that the damage done to the beam at each resonance depends on the speed with which the resonance is crossed. By increasing the acceleration rate, the resonance is crossed faster and thus the damage inflicted to the beam is reduced.

We have repeated the run of Fig. 1 at an acceleration rate 6.9 G/μsec, which is ten times higher than the rate of the initial run. Results are shown in Fig. 6. The reference electron crossed all the higher than $\ell = 6$ modes without locking in at any of them. However, it acquired substantial peak transverse velocity ($\approx 16\%$), which was reduced to $\approx 8\%$, just before it reached $\ell = 6$. At $t = 98$ μsec the reference electron arrived at the wall with a speed of 0.35 mm/μsec. When the acceleration rate was reduced to 5 G/μsec, the reference electron locked in at $\ell = 9$, while at 4 G/μsec the ℓ value increased to $\ell = 15$.

E. Effect of additional field errors

We have briefly investigated the effect of additional field errors on the beam lifetime. Initially, we included the contribution from the buswork current feeds. In the experiment, the transitions from coaxial buswork to the vertical field hoops are not circular arcs of the same radius as the coils but are instead straight chords. Analysis [11] of these feeds has shown that they produce field disturbances with amplitude that is several percent of the vertical field. We repeated the run shown in Fig. 1 with the addition of the field errors produced by the feeds. The results indicate that the beam centroid enters the lock-in regime at $\ell = 24$ and the beam lifetime is reduced by 30%.

Furthermore, we have studied the effect of field errors that arise from the discreteness of the toroidal field coils. Instead of a smooth toroidal magnetic field that varies as $1/r$, the field is computed from the Biot-Savart law for 12 rectangular shape coils of infinitesimal minor radius. The remaining dimensions and positions are the same as those of the experiment. The field errors from the discreteness of the toroidal field coils gave almost identical results with the error from the feeds.

IV. DISCUSSION

This paper addresses the effect of random fluctuations of stellarator windings on the dynamics of the beam centroid in a MBA configuration.

Our results show that random displacement of the windings by more than ± 0.5 mm produce field errors that excite the cyclotron resonance modes that efficiently direct most of the input energy from the axial to transverse direction. These random displacements become completely harmless when their maximum amplitude is reduced to ± 0.5 mm. It should be noticed that the NRL

group already constructed a strong focusing system with the windings positioned with an accuracy of ± 0.5 mm.

In addition to more accurate positioning of the windings, the effect of random fluctuations on the beam dynamics becomes benign either by using a crowbar on the current of the windings, before the critical resonance is reached, or by enhancing the accelerating rate. Therefore these fluctuations are not critical to the MBA, but affect its cost.

Finally, at $\ell = m$ (≈ 6 in our case), where ℓ is the value of the cyclotron mode and m is the value of field periods in the device, i.e., when the frequency of the cyclotron mode is equal to the frequency of the strong focusing mode, the beam centroid encounters a potent resonance and locks in at it, even when the windings are located at their ideal positions. If crossing of the $\ell = m = 6$ mode is desired, using a crowbar on the strong focusing field appears to be the only remedy.

APPENDIX

This appendix provides a brief outline of the numerical model used to study the effect of random fluctuations of stellarator windings on the dynamics of the beam centroid in a MBA configuration.

The code employs the cylindrical coordinate systems as shown in Fig. 7. The global system $\hat{e}_r, \hat{e}_\theta, \hat{e}_z$ has its origin at the intersection of the midplane of the torus with the major axis and its $\hat{e}_z$ axis is along the major axis of the torus. The local coordinate system $\hat{e}_x, \hat{e}_y, \hat{e}_s$ has its origin on the minor axis.

The instantaneous position of the beam centroid in the vertical plane is

$$r = r_0 + X,$$

$$z = Z,$$

where X and Z are its coordinates in the local system.

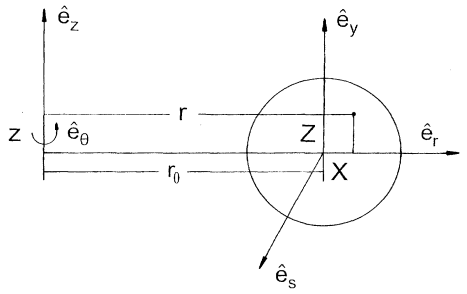

FIG. 7. Systems of coordinates.

The equations of motion in the $\hat{e}_x, \hat{e}_y, \hat{e}_s$ system for the reference electron that is located at the centroid of a circular cross section electron beam are

$$\frac{d(\gamma v_r)}{dt} = \frac{v_\theta^2 \gamma}{r} - \frac{e}{m_e}\left(E_r + \frac{1}{c}(v_\theta B_z - v_z B_\theta)\right), \quad \text{(A1)}$$

$$\frac{d(\gamma r v_\theta)}{dt} = -r\frac{e}{m_e}\left(E_\theta + \frac{1}{c}(v_z B_r - v_r B_z)\right), \quad \text{(A2)}$$

$$\frac{d(\gamma v_z)}{dt} = -\frac{e}{m_e}\left(E_z + \frac{1}{c}(v_r B_\theta - v_\theta B_r)\right), \quad \text{(A3)}$$

where $\gamma = [1 + \frac{1}{c^2}(P_r^2 + P_\theta^2 + P_z^2)]^{1/2}$ is the relativistic factor and $P_r = m_e \gamma v_r$, $P_\theta = m_e \gamma v_\theta$, $P_z = m_e \gamma v_z$ are the three components of the momentum.

The above system of differential equations is solved with the aid of a fourth order Runge-Kutta method using a set of initial values for γ, r, z, v_r, v_z, and v_θ.

The components B_r, B_z, B_θ of the total magnetic field acting on the reference electron are calculated at its position as described in Sec. II. The induced accelerating component E_θ of the electric field is calculated from the time varying vertical magnetic field.

[1] P. Sprangle and C. A. Kapetanakos, J. Appl. Phys. **49**, 1 (1978).
[2] R. L. Gluckstern (unpublished).
[3] C. Roberson, A. Mondelli, and D. Chernin, Phys. Rev. Lett. **50**, 507 (1983).
[4] D. Kerst, Phys. Rev. **60**, 47 (1941).
[5] C. A. Kapetanakos *et al.*, Phys. Rev. Lett. **61**, 86 (1988).
[6] C. A. Kapetanakos *et al.*, Phys. Fluids B **5**, 2295 (1993).
[7] H. Ishizuka *et al.* (unpublished).
[8] D. Dialetis, S. J. Marsh, and C. A. Kapetanakos, Phys. Rev. E **47**, 2043 (1993).
[9] C. A. Kapetanakos *et al.*, NRL Report No. NRL/MR/6793-92-7161 (unpublished) (see Fig. 21).
[10] C. A. Kapetanakos, P. Sprangle, S. J. Marsh, D. Dialetis, C. Agritelis, and A. Prakash, Part. Accel. **18**, 73 (1985) (Eqs. 36 and 37).
[11] J. Golden *et al.*, Proc. SPIE **1407**, 418 (1991).